

# Energy and Exergy Analyses Applied to a Crop Plant System

Heba Alzaben <sup>1,\*</sup> and Roydon Fraser <sup>2,\*</sup>

<sup>1</sup> Department of Mechanical Engineering, Faculty of Engineering, AlHussein Technical University, Amman 11942, Jordan

<sup>2</sup> Department of Mechanical and Mechatronics Engineering, University of Waterloo, Waterloo, ON N2L 3G1, Canada

\* Correspondence: heba.alzaben@htu.edu.jo (H.A.); rafraser@uwaterloo.ca (R.F.)

**Abstract:** The second law of thermodynamics investigates the quality of energy, or in other words exergy, described as the maximum useful to the dead-state work. The objective of this paper is to investigate the energy and exergy flows in a crop plant system in order to identify the dominant flows and parameters (e.g., temperature) affecting crop plant development. The need for energy and exergy analyses arises from the hypothesis that crop stress can be detected via surface temperature measurements, as explained by the exergy destruction principle (EDP). Based on the proposed energy model, it is observed that radiation and transpiration terms govern all other terms. In addition, as a result of exergy analysis, it is observed that solar exergy governs all input and output terms. The results obtained from this study support the hypothesis that crop surface temperature can be utilized as an indicator to detect crop stress.

**Keywords:** crop stress detection; exergy destruction principle; crop plant energy balance; crop plant exergy balance; transpiration; solar exergy

## 1. Introduction

The first law of thermodynamics, the energy conservation law, discusses the quantity of energy in a process. It states that energy can neither be created nor destroyed, but it is a conserved quantity [1], according to which it can only be transformed from one form to another. As an example, in a crop plant system, the incoming solar energy is converted into chemical energy during a photosynthesis process [2]. Different models have been developed to study the energy balance in a crop plant system, taking into consideration the system boundary variation; most of the models have focused on the evaluation of sensible heat flux (H), latent heat flux (LE), and soil conduction (G) [3,4], usually derived from eddy covariance (EC) flux measurement towers [5], which is considered the most direct method to monitor energy fluxes. On the other hand, the second law of thermodynamics describes the changes in the quality of energy, otherwise known as exergy, in a process. It is the driving force behind living systems and self-organization; exergy destruction is directly proportional to entropy production, according to the Gouy–Stodola theorem [1]. The second law of thermodynamics explains the relationship between temperature and entropy; when a system is involved in an irreversible process, entropy will be produced, and exergy will be destroyed.

Entropy production is an implicit form of exergy analysis, according to the Gouy–Stodola theorem, ( $\dot{X}_{destroyed} = T_0 \times \dot{S}_p$ ) [6,7], where  $\dot{X}_{destroyed}$  is the level of exergy destruction,  $T_0$  is the temperature of the environment, and  $\dot{S}_p$  is the amount of entropy production. Exergy is used in this regard as opposed to energy and entropy due to its three main properties:



Academic Editor: Johan Jacquemin

Received: 29 October 2024

Revised: 9 January 2025

Accepted: 22 January 2025

Published: 30 January 2025

**Citation:** Alzaben, H.; Fraser, R. Energy and Exergy Analyses Applied to a Crop Plant System. *Thermo* 2025, 5, 3. <https://doi.org/10.3390/thermo5010003>

**Copyright:** © 2025 by the authors. Licensee MDPI, Basel, Switzerland. This article is an open access article distributed under the terms and conditions of the Creative Commons Attribution (CC BY) license (<https://creativecommons.org/licenses/by/4.0/>).

context-sensitive, universal, and not conserved property. First, exergy is context-sensitive because it is formulated with respect to a reference environment [8–10]. In addition, when a system is subject to a thermodynamic equilibrium with its surroundings, it will have zero exergy [11]. Second, exergy is a universal property, according to which all thermodynamic systems are compared based on their exergy content [7]. Third, unlike energy, it cannot be created or conserved, but only destroyed, during an irreversible process [8,12,13]. Due to its properties, exergy is used as a decision-making and optimization tool in many engineering applications, such as power plant design and operation specifications [14], and it is also used in many non-engineering applications, including ecology [15–17], life cycle assessments [18,19], resource accounting [8,20,21], biology, sustainability [15,16,22], and as a health assessment tool in terms of an ecosystem [23]. Exergy is preferred over entropy because it has the same units of measurement (e.g., kJ) as the units of entropy (e.g., kJ/K). For example, exergy can be considered the ability to lift a weight. It is fundamental to the exergy destruction principle for ecosystems [15–17,24–31], and it has a well-defined maximum compared to entropy production.

The main difference between exergy and Gibbs free energy lies in their reference frameworks; exergy quantifies the amount of work an energy carrier can perform relative to its surroundings rather than describing an isobaric process involving the energy carrier and a reference state [32]. Gibbs free energy represents the maximum amount of work that a system can perform under constant temperature and pressure conditions, which has wide applications in engineering, particularly in terms of investigating the relevant chemical reaction and phase change-related problems [33]. Exergy represents the theoretical maximum work potential within a given environment rather than the actual work achievable with the existing technology.

Many researchers have made significant contributions in the field of exergy when applied to ecological and agricultural systems. Szargut [34] proposed integrating exergy analysis with ecological concepts to investigate the interactions between human activities and natural systems. In addition, the cumulative exergy consumption (CExC) of non-renewable natural resources was introduced, which was utilized to assess various energy limitations in the crop production process [35]. It is defined as the total exergy of all the resources utilized and consumed throughout the supply chain of a specified product or process [36]. Furthermore, Szargut [37] applied exergy principles to agricultural systems to evaluate the energy efficiency of crop production. His work focused on analyzing the balance between inputs (e.g., sunlight, fertilizers, water) and outputs (e.g., biomass, yield) to identify opportunities for crop yield optimization. Orrego et al. [38] applied exergy analysis to complex systems, such as biological systems, which included assessing exergy destruction in regard to living organisms. It was found that the exergetic efficiency of plant vegetation is notably low [38]. Many researchers have adopted Szargut's methodology in calculating the physical and chemical exergy of crop plant systems. Furthermore, Pimentel focused on the input–output analysis of agricultural production systems, with the aim of demonstrating its ongoing relevance to address complex environmental issues [39], including soil erosion, the loss of biodiversity, and biofuel and biomass energy-related problems. Pimentel and Patzek [40] suggested that living systems can sustain themselves and reproduce if they successfully acquire what they define as “energy input” (exergy within a well-defined system) and eliminate what they classify as “waste” (degraded energy). This concept was further developed and refined by the Prigogine school of thought [41–43] through advancement in non-equilibrium thermodynamics. Righetto and Mady [44] conducted an exergy analysis of sun–plant interactions in sugarcane cultivation using mathematical models to estimate plant production and exergy flows while evaluating photosynthetic efficiency. Their findings revealed that exergy

efficiency varies significantly with seasonal changes. Jekayinfa et al. [45] investigated the exergy analysis of soybean production in Nigeria. It was found that the exergy-to-energy ratio of certain inputs, such as potassium and phosphorus, exceeded unity. Nikkhah et al. [46] explored the impact of variety selection on the exergy flow within a paddy rice production system. Nine varieties of rice were assessed in Italy using the cumulative exergy analysis method. It was found that fossil fuels and chemical fertilizer accounted for the highest consumption relative to total energy consumption across all varieties.

Two hypotheses have been developed to detect crop stress at early growth stages before any visible signs appear on the plant surface [47–49]. The first hypothesis posits that crops exhibiting greater growth and higher yield will have lower daytime surface temperatures compared to less developed crops. The second hypothesis asserts that stressed crops will have higher surface temperatures during the day compared to less stressed crops and lower surface temperatures at night to maintain the net energy balance assumption. The exergy destruction principle (EDP) was used as a theoretical framework to explain the anticipated inverse relationship between crop surface temperature and crop stress [48]. Thermal remote sensing was employed through crop surface temperature measurements and spectral emissivity calculations to test the two hypotheses under greenhouse and variable field conditions. The results confirmed at a 0.05 significance level that stressed and less developed crops have higher surface temperatures during the day compared to less stressed and more developed crops. Therefore, it is important to investigate energy and exergy models using the two main thermodynamics principles (i.e., first and second laws) and apply them to a crop plant system—corn, for instance, as discussed in this paper. According to the first law of thermodynamics, cooler surfaces emit less radiation at a lower exergy level into the atmosphere compared to warmer surfaces [17,24,26]. Consequently, a system will gain more exergy, as suggested by the second law of thermodynamics. Thus, crop surface temperature reflects the efficiency of the first and second laws of thermodynamics. This paper focuses on energy and exergy balance models, employing different sets of assumptions to simplify the equations and analyze various input and output terms (e.g., fertilizer input, soil conduction flux, water transpiration, biomass output, etc.) to identify the largest contributing factors and confirm the use of surface temperature as an indicator for crop stress detection from an exergy balance perspective.

A crop plant system can be modeled as a black box with input and output energy flow from an engineering thermodynamic perspective [47–49], where all physiological processes and mechanisms involved in regulating crop surface temperature, including transpiration, evapotranspiration, stomatal conductance, and photosynthesis, are considered [48]. Variations in crop surface temperature, as predicted by the exergy destruction principle (EDP), are primarily influenced by the development processes occurring during the early growth stages of corn plants [47,48]. Environmental conditions must remain consistent across systems when comparing crop plants supplied with different nutrient levels using the exergy destruction principle. This means nutrient availability is treated as an internal factor within the “black box”. This approach allows for an EDP-consistent comparison between crops supplied with varying nutrient levels [47–49]. The exergy destruction principle (EDP) operates as a “black box” model that disregards internal system mechanisms, such as respiration, and focuses exclusively on energy flow at the system boundary. In the context of non-equilibrium thermodynamics for complex systems, such as crop–plant systems or ecosystems, exergy serves as a measure of the deviation between the system and its environment from thermodynamic equilibrium, which is driven by an externally applied gradient such as temperature or pressure. Consequently, both the system and its environment must be well defined. Exergy is a valuable tool for analyzing non-equilibrium thermodynamic systems; higher exergy levels indicate a greater deviation from equilib-

rium. The exergy destruction principle, as defined by James Kay [17,26], states “A system subjected to an external flow of exergy will be displaced from its equilibrium state. In response, the system will reorganize itself to degrade exergy as effectively as possible under the given conditions, thereby minimizing the extent of its deviation from thermodynamic equilibrium. Moreover, the further the system is displaced from equilibrium, the greater the number of organizational (i.e., dissipative) opportunities that become available, which result in increased efficiency in the amount of exergy being destroyed”. The further the system is displaced from its equilibrium state, the greater the destruction of exergy and the production of entropy, which means that more work is needed to maintain the system in its non-equilibrium state [15,48]. The exergy destruction principle (EDP) hypothesis states that ecosystem development is related to optimizing the available work required for organization, structure, function, and survival, thereby enhancing the ecosystem’s capacity to destroy the incoming solar exergy. Ecosystems are complex, non-equilibrium, self-organizing, dissipative thermodynamic systems that are open to energy and mass flows, maintaining their organization and structure through continuous energy dissipation. As ecosystems evolve and mature, their total energy dissipation and utilization of available exergy increase, leading to the development of more complex structures with greater diversity [17,26]. This development allows ecosystems to adapt to their environment while enhancing their capacity to capture and utilize solar exergy from the incoming radiation to sustain their organization. The greater the exergy being captured, the stronger the ecosystem’s ability to support organizational processes. Consequently, the progression of ecosystem development is quantified by its rate of exergy utilization [17,26]. Exergy, unlike entropy, indicates how far from equilibrium a system is, the magnitude of the gradients, and the potential of the system to perform useful work [15,16].

For more details on how this EDP principle is applied to a crop plant system, please refer to our longer work in [47–49]. Conducting energy and exergy analyses for a crop plant involves evaluating the energy and exergy flows within the various processes associated with cultivation, harvesting, and processing. For energy input analysis it is important to consider the amount of energy received from the sun during the growth period, which is crucial for photosynthesis. In addition, it is important to include the energy used in production, transportation, and application of fertilizers, as well as the energy required for irrigation. For the energy output analysis, it is essential to include the biomass which evaluates the energy content of the harvested plant considering both grain and plant residues. On the other hand, exergy is a measure of energy quality, defined as the maximum useful work achievable relative to the dead state [24]. Exergy analysis considers not only the quality of energy but also the irreversibilities in different processes. For a crop plant, it is important to evaluate the exergy content of input and output flows through the system boundary, including solar, water, and nutrient exergy as inputs, and biomass as the output. Solar, water, and nutrient exergy as input, and biomass as output. Exergy analyses are vital for decision-making tools for analyzing, comparing, and simulating different thermal systems. The objective of this paper is to investigate the energy and exergy flows in a crop plant system to identify the dominant flows and parameters (e.g., temperature) affecting crop plant development. Additionally, several opportunities for developing the proposed exergy analysis are explored.

#### *Crop Surface Temperature Measurement Considerations*

The two hypotheses developed to detect crop stress at early growth stages [47–49] were tested under greenhouse and field conditions. For field experiments, soil nitrate samples were collected from a depth of 30 cm multiple times: before planting and after harvesting the field to investigate the residual nitrogen content in the soil from the previous year. The

same plots were used to examine the variation in nitrate levels in the soil. Five cores per plot were collected and combined. A non-significant difference in soil nitrate was observed among different nitrogen treatments within the field before fertilizer application each year; this finding implies that the amount of nitrogen applied in the previous year does not impact soil nitrate levels in the subsequent year. For greenhouse experiments, soil nitrate content was measured using a colorimeter (Smart 3 Soil, LaMott, MD, USA), which showed that soil nitrate content increases with nitrogen rate supply.

In regard to water content, the volumetric water content (i.e., the ratio of the water volume to soil volume) was measured across various plots within the field using an EC5 soil moisture sensor (Decagon Devices, Inc., Pullman, WA, USA), which was installed at a depth of 10 cm below the ground surface. Corn plants were monitored for water stress conditions throughout the growing seasons of 2016, 2017, 2018, and 2019 with concurrent measurements of soil volumetric water content and precipitation rates [47,48]. For example, in 2018, the volumetric water content for plots receiving 0 and 188 kg N ha<sup>-1</sup> was 18.46 ± 0.058% and 16.33 ± 0.038% (m<sup>3</sup> m<sup>-3</sup>), respectively, based on 10-day averages across four plots per nitrogen rate [48]. These values fall within the field capacity range of 22% to 28% for silt clay loam soil [50]. Additionally, the absence of visible wilting in the plants suggests that corn plants did not experience significant water stress [47].

The measured crop surface temperatures were corrected for meteorological conditions on different days, as variations in air temperature affect the sensitivity of crop surface temperature measurements. The following equation was used for the crop surface temperature correction:

$$T_{c\_c} = T_c - T_a + T_{a\_mean} \quad (1)$$

where  $T_c$  is the canopy temperature (°C),  $T_a$  is the air temperature (°C), and  $T_{a\_mean}$  is the mean air temperature (°C).

It was observed that the corn surface temperature decreased with increasing nitrogen application rates. A consistent, statistically significant ( $p$ -value < 0.05) negative correlation was identified between the crop surface temperature and applied nitrogen rate. However, surface temperature measurements showed variability due to external and weather-dependent factors that influence crop surface temperature. Figure 1 below summarizes the mean surface temperature as influenced by the nitrogen application rate during June and July 2017. The regression analysis consistently identified a negative slope [47,48].

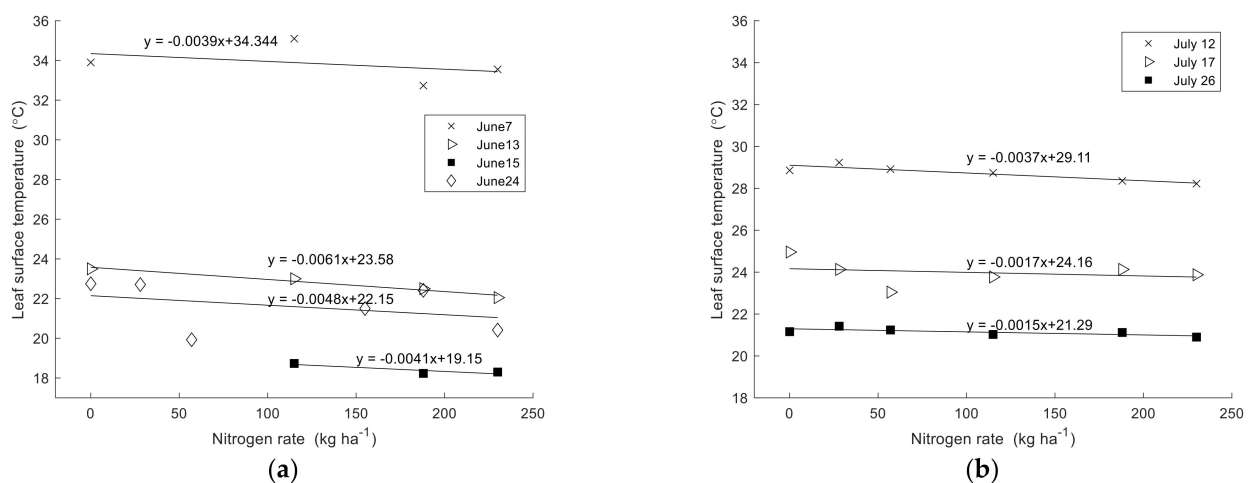


**Figure 1.** The mean leaf surface temperature as influenced by nitrogen application rate is shown for (a) June 2017 and (b) July 2017. Each data point represents the daily average of 12 temperature measurements, which were derived from three measurements per replication across four replications for each nitrogen rate (adapted from [47]).

Sensitivity analyses were conducted to assess the impact of various input variables on the output (i.e., crop surface temperature). The findings indicated that the non-stress-related variables such as variations in solar irradiance, air temperature ( $T_{\text{air}}$ ), soil temperature ( $T_{\text{soil}}$ ), vapor pressure deficit (VPD), soil moisture ( $\text{Soil}_{\text{moist}}$ ), relative humidity (RH), wind speed ( $V$ ), time of the day ( $t$ ), cloud cover (CC), crop genetics, leaf angle ( $\theta$ ), leaf emissivity ( $\epsilon$ ), and sensor view angle require further control or compensation through conditional sampling. This approach would enhance confidence in the results when investigating the relationship between crop stress and crop surface temperature under variable conditions [48].

## 2. Materials and Methods

### 2.1. Energy Balance Applied to Crop Plant System

The exergy destruction principle described above is associated with the black-box concept of thermodynamics to evaluate the use of crop surface temperature in characterizing energy flow within a crop plant system. A crop plant system is modeled as a black box with input and output energy and mass flows as presented in Figure 2 [48,49]. The system boundary is defined by the dashed line in Figure 2 and includes plants and part of the soil. For mass flow, water enters the system through the soil, rainfall, or irrigation and exits via soil evaporation and plant evapotranspiration. Fertilizer is introduced into the system through controlled applications at specified times with biomass serving as the mass output. Airflow into and out of the system carries water vapor, while the soil conducts thermal energy into or out of the system. Solar radiation that reaches the crop surface is either absorbed or reflected with additional background radiation emitted by atmospheric molecules and adjacent objects.

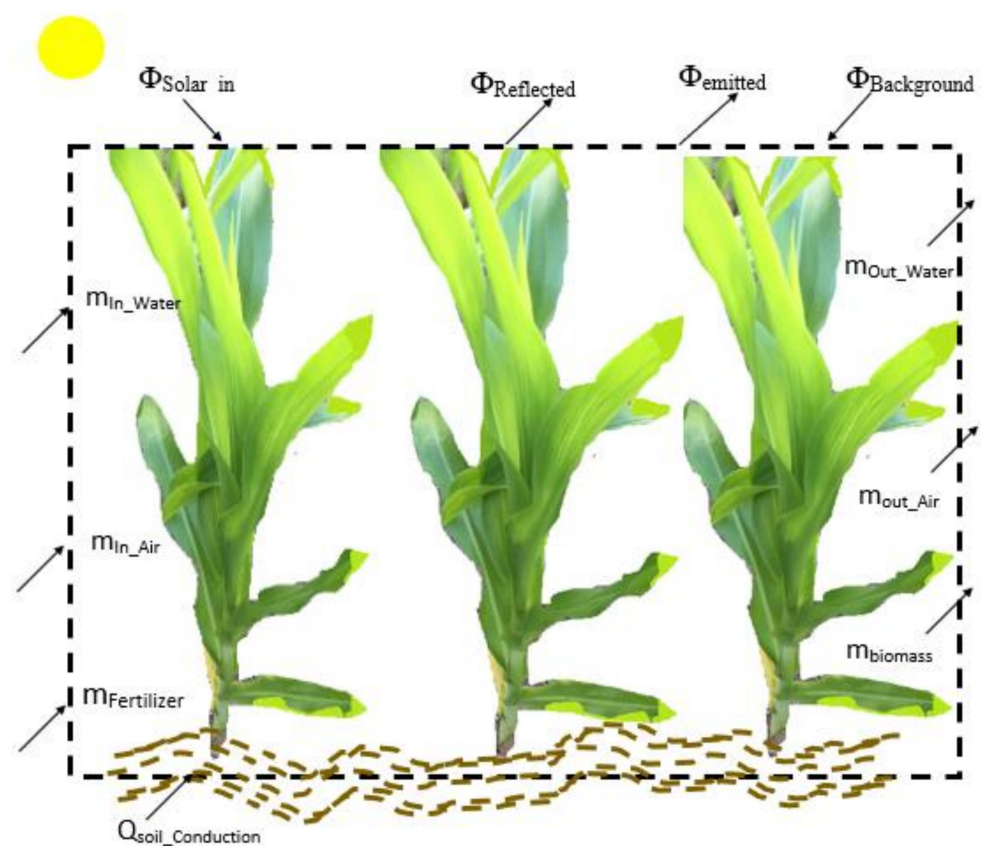


Figure 2. Energy and matter flow for a crop plant system [47–49].

The first law of thermodynamics energy balance equation for an open thermodynamic system such as a crop plant system is presented in Figure 1 with matter and energy flows across the system boundary given by

$$\frac{dE}{dt} = \dot{\Phi}_{Solar\_in} + \dot{\Phi}_{Background} + \dot{\Phi}_{Reflected} + \dot{\Phi}_{emitted} + \dot{Q}_{Soil\_conduction} + \int PdV \dot{m}_{in} \left( h + \frac{v^2}{2} + gz \right)_{in} - \dot{m}_{out} \left( h + \frac{v^2}{2} + gz \right)_{out} \quad (2)$$

where

|                              |   |
|------------------------------|---|
| $\frac{dE}{dt}$              | the rate of change in the system energy.                  |
| $\dot{E}_{in}$               | energy input into the system.                             |
| $\dot{E}_{out}$              | energy output from the system.                            |
| $\dot{\Phi}_{Solar\_in}$     | solar radiation input.                                    |
| $\dot{\Phi}_{Reflected}$     | reflected radiation.                                      |
| $\dot{\Phi}_{Background}$    | background radiation.                                     |
| $\dot{\Phi}_{emitted}$       | emitted radiation.  |
| $\dot{Q}_{Soil\_conduction}$ | soil conduction heat flux.                                |
| P                            | atmospheric pressure.                                     |
| h                            | Specific enthalpy of the crop plant system.               |
| V                            | system volume.  |
| v                            | system velocity.  |
| g                            | gravitational acceleration.                               |
| z                            | system height.  |
| $\dot{m}_{in}(out)$          | mass flow input (output) to (from) the crop plant system. |

The energy balance equation for a crop plant system is established, and various energy flow terms are presented in Equation (2). However, it is important to analyze the order of magnitude for energy terms to identify the dominant energy term required for the development of a crop plant system.

Base Assumption: Case Study for Ontario, Canada

In order to estimate the magnitude of different energy terms and flows in the energy balance Equation (2), a temperate zone agriculture location was selected to represent an average scenario. Section 2.2 below utilizes the Elora, Ontario, Canada case study location as needed. For radiation terms, measurements were taken using a net radiometer (Apogee instrument SN-500-SS, Logan, UT, USA) at Elora, Ontario, Canada during clear-sky conditions on various days in 2019 [47,48]. It was observed that the incoming solar radiation was between 400 and 900 W /m<sup>2</sup>, reflected radiation was between 80 and 120 W /m<sup>2</sup>, background radiation was between 350 and 500 W /m<sup>2</sup>, and emitted radiation was between 400 and 700 W /m<sup>2</sup>. For more details, please refer to our longer work in [47,48].

## 2.2. Energy Flow Terms Estimation

This section outlines the order of magnitude estimates for the energy-related components described in Equation (2). Through this analysis, primary terms necessary for a first-order analysis are identified along with secondary terms relevant to more detailed analyses.

### 2.2.1. Air Expansion

As an example, consider a 2-m-high volume above ground as in the system shown in Figure 3. For simplicity in calculation, a surface area of 1 m<sup>2</sup> is considered, as illustrated in Figure 3b. While the system boundary volume is fixed by definition, as the air heats up during the day, it expands, causing some air to exit in the system while carrying energy with it. To estimate the magnitude of energy loss due to air expansion, it is assumed that

air leaves in the perpendicular direction, as presented in Figure 3a. Additionally, it is assumed that the entire volume is filled with air to provide a conservative estimate of the energy flow.

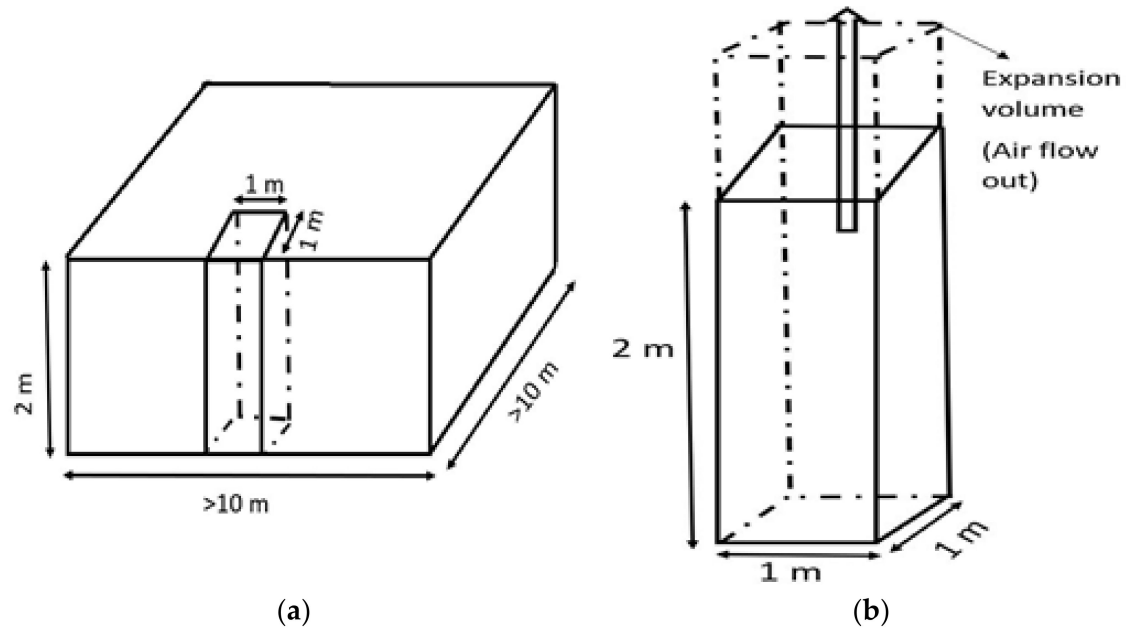


**Figure 3.** Air expansion model: (a) field dimensions, (b) expansion volume, air flow output (From [48]).

Considering an initial volume of  $2 \text{ m}^3$  of air as presented in Figure 3b at  $10 \text{ }^\circ\text{C}$ , and assuming constant pressure at  $100 \text{ kPa}$ , an increase in temperature by  $20 \text{ }^\circ\text{C}$  results in a final temperature of  $30 \text{ }^\circ\text{C}$ . Using the ideal gas equation, the air density decreases, causing the air to expand. This expansion results in  $0.14 \text{ m}^3$  of air exiting the system. The energy transported outside the system is given by

$$E_{\text{out}} = m_{\text{out}} C_p \Delta T \quad (3)$$

The mass output ( $m_{\text{out}}$ ) is  $0.167 \text{ kg}$  (calculated using the ideal gas equation) and the energy output ( $E_{\text{out}}$ ) is  $3.35 \text{ kJ}$ , as determined from Equation (3). The specific heat capacity of air ( $C_p$ ) is  $1.007 \text{ kJ/kg }^\circ\text{C}$ . The energy output rate over a 4-h period, given a temperature difference ( $\Delta T$ ) of  $20 \text{ }^\circ\text{C}$ , is  $0.23 \text{ W}$ . This value is considered negligible compared to the measured midday radiation components in the Elora field, ON, Canada, where crop surface temperature was measured using a thermal camera [47,48].

### 2.2.2. Water Expansion

Using the same methodology applied to estimate the order of magnitude for air expansion. The water expansion discussed in Equation (2) is also negligible. Assuming that the entire  $2 \text{ m}^3$  of volume illustrated in Figure 3b is filled with water vapor at  $100 \text{ kPa}$  with a temperature change from  $10 \text{ }^\circ\text{C}$  to  $30 \text{ }^\circ\text{C}$ , the expansion volume will remain the same at  $0.14 \text{ m}^3$ . However, the output mass ( $m_{\text{out}}$ ) is  $0.104 \text{ kg}$ , and because gas constant ( $R$ ) and specific heat capacity ( $C_p$ ) differ for water vapor, the amount of energy output from Equation (3) is  $3.89 \text{ kJ}$ , and the rate of energy output over a 4-h period, as the water warms from  $10 \text{ }^\circ\text{C}$  to  $30 \text{ }^\circ\text{C}$ , is  $0.27 \text{ W}$ . This value is also negligible compared to the measured midday radiation components.

### 2.2.3. Water Transpiration

Various researchers have investigated the daily water output of corn plants [51,52] with the maximum amount of water used in calculations reported as 15,100 L per day per acre, assuming an output mass flow of 3.7 L/day /m<sup>2</sup>, which is equivalent to 4.3 × 10<sup>-5</sup> kg/s. Water enters the plant surface in a liquid form and leaves in water vapor form in a transpiration process. The enthalpy change ( $\Delta h$ ) is estimated as follows:

$$\Delta h = C_{p_{liquid}}(T_{in} - T_{leaf}) + h_{fg}(T_{leaf}) + C_{p_{vapour}}(T_{leaf} - T_{out}) \quad (4)$$

Assume an input temperature ( $T_{in}$ ) of 10 °C, a leaf temperature ( $T_{leaf}$ ) of 25 °C, and an output temperature ( $T_{out}$ ) of 30 °C where the specific heat capacity of liquid water ( $C_{p_{liquid}}$ ) is 4.18 kJ/kgK, the specific heat capacity of water vapor ( $C_{p_{water vapor}}$ ) is 1.996 kJ/kg·K, and the latent heat of vaporization ( $h_{fg}$ ) for water at 25 °C is 2442.3 kJ/kg (as per thermodynamic tables). The amount of energy associated with water output due to the transpiration process is calculated to be 102 W (derived from Equation (4)). This energy is significant when compared to the measured midday radiation components at the Elora, ON, Canada location.

### 2.2.4. Biomass Output

The energy associated with biomass output is negligible before harvest when temperature measurements were conducted. However, following harvest, biomass output contributes to the total energy of the crop plant system. For instance, corn cobs and stalks have a high calorific energy value of 17.72 MJ/kg, while corn leaves have a calorific energy value of 16.99 MJ/kg [53]. Assuming five corn plants have a total biomass of 6 kg (based on data collected from greenhouse and field experiments), the estimated total biomass for a field plot area of 60 m<sup>2</sup>, with 600 corn plants over a three-month growing season, is 720 kg. By multiplying this total biomass by its specific energy, the biomass energy output after harvest is calculated to be 26 W, which is minimal compared to the measured midday radiation components. The biomass output accounts for 3% of the incident solar radiation with a maximum incident radiation energy of 900 W/m<sup>2</sup> under clear-sky conditions. No energy gain or loss was observed during the morning and early afternoon due to changes in heat storage within the biomass, which was subsequently released back into the air in the evening hours [54].

### 2.2.5. Soil Conduction Flux

Assuming a depth of 1 m below ground over an area of 1 m<sup>2</sup>, with a temperature difference ( $\Delta T$ ) between the soil and the surface of 35 °C [47–49], and a soil temperature of 10 °C, the thermal conductivity ( $k$ ) of the Elora soil is 0.5 W/mK [55]. The conduction heat flux is calculated to be 7.5 W/m<sup>2</sup> as follows:

$$Q_{soil\_conduction} = \frac{-k\Delta T}{L} \quad (5)$$

The conduction heat flux ( $Q_{soil\_conduction}$ ) is small compared to the measured midday radiation components in the Elora, Ontario, Canada location.

## 2.3. Exergy Balance Applied to a Crop Plant System

As previously discussed, and illustrated in Figure 2, surface temperature can serve as the sole measurement to determine the net amount of exergy available to a crop plant system under the black box framework. The exergy balance equation is presented as follows:

$$\frac{dX}{dt} = \dot{X}_{in} - \dot{X}_{out} - \dot{X}_{Destroyed} \quad (6)$$

Equation (6) can be expanded as follows:

$$\frac{dX}{dt} = \dot{X}_{solar\_in} + \dot{X}_{Background} + \left(1 - \frac{T_0}{T_{soil}}\right) \dot{Q}_{Soil\_conduction} + \int PdV + \dot{m}_{in}\psi_{in} - \dot{X}_{Reflected} - \dot{X}_{Emitted} - \dot{m}_{out}\psi_{out} - \dot{X}_{Destroyed} \quad (7)$$

where:

|                        |   |
|------------------------|---|
| $\frac{dX}{dt}$        | the rate of exergy changes in the crop plant system.                                |
| $\dot{X}_{in(out)}$    | input (output) exergy to (from) the crop plant system.                              |
| $\dot{X}_{Destroyed}$  | exergy destroyed due to reversibilities.  |
| $\dot{X}_{Solar\_in}$  | exergy associated with incoming solar radiation.                                    |
| $\dot{X}_{Reflected}$  | exergy associated with reflected radiation.   |
| $\dot{X}_{Background}$ | exergy associated with background radiation.  |
| $\dot{X}_{Emitted}$    | exergy associated with emitted radiation.   |
| $T_0$                  | reference environment temperature of 30 °C for the Elora, Ontario, Canada location. |
| $T_{Soil}$             | soil temperature of 10 °C.  |
| $\psi_{in(out)}$       | specific exergy input (output) to (from) a crop plant system.                       |

The exergy balance equation is established, and various exergy flow terms are outlined in Equation (7). However, it is essential to examine the order of magnitude of these exergy terms to identify the most dominant ones critical for crop plant system health and development.

#### 2.4. Exergy Flow Terms Estimation

This section examines the order of magnitude ratio estimates for different exergy flow terms relative to solar exergy flow.

##### 2.4.1. Exergy Associated with Solar Energy

For solar exergy calculations, there is ongoing debate regarding three models used to determine solar exergy, which each rely on a different set of assumptions. The solar exergy represents the maximum theoretical work that can be extracted from incident solar radiation. The debate exists because it is not clear which set of assumptions is most appropriate. The first model depends on incident solar radiation flux and surface temperature, in which no entropy production and a specified area are assumed, and it does not account for system geometry, size, or any structural considerations. The second model assumes entropy production and a specified area [24]. The third model assumes no entropy production with a non-specified area. In this paper, Model 1 from Kabelac [55] is used to calculate solar exergy. This model represents a real system that has a finite area, and the zero entropy production assumption is consistent with the zero entropy production of Carnot heat engine assumption. The equation for solar exergy,  $X_{solar}$ , based on Model 1 is as follows:

$$\frac{X_{solar}}{\Phi_{solar}} = \left[ 1 - \frac{4}{3} \frac{T_{surface}}{T_{solar}} + \frac{1}{3} \frac{T_{surface}^4}{T_{solar}^4} \right] \quad (8)$$

where

|                |  |
|----------------|--|
| $X_{solar}$    | solar exergy.                                |
| $\Phi_{Solar}$ | incoming solar energy.                       |
| $T_{Surface}$  | crop surface temperature (assumed of 25 °C). |
| $T_{Solar}$    | solar temperature of 5762 K [24].            |

The incident solar energy measured using a net radiometer on various days in 2019 at the Elora, ON, Canada location [47,48] ranged between 400 and 900 W/m<sup>2</sup>. The solar

exergy ratio ( $\frac{X_{solar}}{\phi_{solar}}$ ) was calculated as 0.931 with the corresponding solar exergy ( $X_{solar}$ ) values ranging from 370 to 838 W/m<sup>2</sup>.

#### 2.4.2. Exergy Associated with Background Radiation

The exergy associated with background radiation is estimated using Equation (8), substituting the background temperature ( $T_{Background}$ ) for the solar temperature ( $T_{Solar}$ ). For clear-sky conditions, the background temperature is assumed to be  $T_{Background} = 1$  °C, while for cloudy conditions,  $T_{Background} = 18$  °C [56]. Based on Model 1 [55], the exergy of background radiation is expressed as follows:

$$\frac{X_{Background}}{\phi_{Background}} = \left[ 1 - \frac{4}{3} \frac{T_{surface}}{T_{background}} + \frac{1}{3} \frac{T_{surface}^4}{T_{background}^4} \right] \quad (9)$$

The background exergy ratio ( $\frac{X_{Background}}{\phi_{Background}}$ ) is 0.0163 for  $T_{background} = 1$  °C and 0.01173 for  $T_{background} = 18$  °C. Figure 4 illustrates the decrease in the background exergy ratio as the background temperature increases. This indicates that cloudy days, which are characterized by higher background temperatures, result in a lower exergy ratio compared to clear-sky conditions. The background radiation ( $\Phi_{background}$ ) measured using a net radiometer on various days in 2019 at the Elora, ON, Canada location [6,7] ranged between 350 and 500 W/m<sup>2</sup>. For  $T_{Background} = 1$  °C, the background exergy ( $X_{Background}$ ) was between 5.7 and 8.2 W/m<sup>2</sup>, while for  $T_{Background} = 18$  °C, it ranged from 0.4 to 0.6 W/m<sup>2</sup>. The relative background exergy values were 0.012 for  $T_{Background} = 1$  °C and  $8.28 \times 10^{-4}$  for  $T_{Background} = 18$  °C. These results demonstrate that the exergy associated with background radiation is relatively small. For clear-sky conditions ( $T_{Background} = 1$  °C), it contributes 1.2% of the solar exergy, while for cloudy conditions ( $T_{Background} = 18$  °C), it is negligible, amounting to only 0.0828% of the solar exergy.

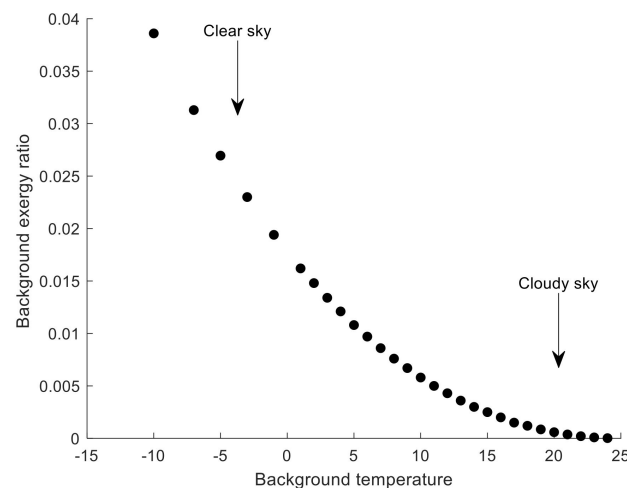


**Figure 4.** Background exergy ratio variation with background temperature.

#### 2.4.3. Exergy Associated with Fertilizer

The exergy associated with fertilizer input is calculated based on the average solar and background radiation flux at the Elora, ON, Canada location, which is 1325 W/m<sup>2</sup> [57]. This value is estimated over a surface area of 1 m<sup>2</sup>, during a three-month growing season with 10 h of sunlight per day. Using ammonium nitrate (UAN) –28% as the fertilizer, which is injected annually between rows, the total solar energy is calculated as follows:

$$1325 \text{ W} \times 3 \text{ months} \times 30 \text{ (day/month)} \times 10 \text{ (h/day)} \times 60 \text{ (min/h)} \times 60 \text{ (s/min)} \text{ equals } 4.29 \text{ GJ.}$$

The total fertilizer applied, based on an optimal nitrogen rate of 150 kg N/ha over 1 m<sup>2</sup> surface area, is 0.015 kg (calculated as 150 kg/ha × 1 ha/(10<sup>4</sup> m<sup>2</sup>) × 1 m<sup>2</sup>). The Gibbs free energy of the fertilizer is 2.3 GJ/tonne [58], which corresponds to its chemical exergy. The total exergy associated with fertilizer input is (2.3 GJ/t × 1 ton/1000 kg × 0.015 kg = 3.45 × 10<sup>-5</sup> GJ). When comparing this Gibbs free energy (equivalent to the chemical exergy of the substance) to the solar exergy, the ratio ( $\frac{X_{Fertilizer}}{X_{Solar}}$ ) is 0.8 × 10<sup>-5</sup>, which is negligible in comparison to solar exergy.

Additionally, weed control was performed under field conditions before corn planting using the herbicide Callisto (Mesotrione, Syngenta, Basel, Switzerland) at 0.3 L/ha along with Primextra II Magnum (S-metolachlor and atrazine, Syngenta) at 3.5 L/ha. The total herbicides applied over 1 m<sup>2</sup> surface area is 22.4 × 10<sup>-5</sup> kg [59], which is significantly less than the 0.015 kg of fertilizer input. Consequently, the exergy associated with herbicide input is 5.17 × 10<sup>-7</sup> GJ, which is also negligible when compared to solar exergy.

#### 2.4.4. Exergy Associated with Soil Conduction Heat Flux

Exergy associated with soil heat flux is calculated as follows:

$$\dot{X}_{soil\_conduction} = \left(1 - \frac{T_0}{T_{soil}}\right) \times \dot{Q}_{soil\_conduction} \quad (10)$$

The exergy is calculated as 0.53 W, while the relative soil exergy ( $\frac{X_{Soil\_conduction}}{X_{Solar}}$ ) is 8.77 × 10<sup>-4</sup>, which is insignificant compared to solar exergy.

#### 2.4.5. Air Expansion Exergy

Using the air expansion example discussed in Section 2.2.1 with the same set of assumptions: 1 m<sup>2</sup> area, atmospheric pressure, soil input temperature, and the reference environment temperature, the air expansion exergy is calculated as follows:

$$X_{air\_expansion} = m_{air\_out} \times [(u_{in} - u_0) + p_0(v - v_0) - T_0(S_{in} - S_0)] \quad (11)$$

The entropy and internal energy terms in Equation (10) are expanded using the ideal gas assumption:

$$X_{air\_expansion} = m_{air\_out} \times \left[ C_v(T - T_0) + p_0(v - v_0) - T_0 \left( C_v \ln\left(\frac{T}{T_0}\right) - R \ln\left(\frac{V_0}{V}\right) \right) \right] \quad (12)$$

where:

|                      |  |
|----------------------|--|
| $X_{Air\_expansion}$ | exergy associated with air expansion.                              |
| $u_{in}$             | internal energy input.   |
| $s_{in}$             | the input entropy calculated at the soil temperature of 10 °C.     |
| $u_0$                | internal energy at the reference environment temperature of 30 °C. |
| $s_0$                | entropy at the reference environment temperature.                  |
| $P_0$                | reference environment pressure of 100 kPa.                         |
| $v_0$                | specific volume at the reference environment temperature.          |

The mass of air exiting the system due to expansion, as calculated from the energy balance equation, is 0.167 kg with a corresponding volume change of 0.14 m<sup>3</sup>. Applying this to Equation (12), the air expansion exergy is calculated to be 0.05 kJ. Over a 4-h period, the rate of air expansion exergy is 3.5 × 10<sup>-3</sup> W, and the relative air expansion ( $\frac{X_{Air\_expansion}}{X_{Solar}}$ ) is 5.8 × 10<sup>-6</sup>, which is negligible when compared to solar exergy.

#### 2.4.6. Water Expansion Exergy

Using the water expansion example discussed in Section 2.2.2, the exergy flow per kilogram of air and water vapor, as detailed in Bejan [6], is analyzed.

$$X_{water\_vapour\_mixture} = \left( C_{p,a} + \omega C_{p,v} \right) \times T_0 \left( \frac{T}{T_0} - 1 - \ln \frac{T}{T_0} \right) (1 + \omega) R_a T_0 \ln \frac{P}{P_0} + R_a T_0 \left( \ln \frac{1 + \omega_0}{1 + \omega} + \omega \ln \frac{\omega}{\omega_0} \frac{1 + \omega_0}{1 + \omega} \right) \quad (13)$$

where:

|                             |  |
|-----------------------------|--|
| $X_{water\_vapor\_mixture}$ | exergy associated with water expansion.                    |
| $C_{p,a}$                   | specific heat capacity of the air.                         |
| $w$                         | specific humidity.   |
| $w_0$                       | specific humidity at the reference environment conditions. |
| $C_{p,v}$                   | specific heat capacity of the water vapor.                 |
| $T$                         | water input temperature of 10 °C.                          |
| $\omega$                    | mole fraction ratio.                                       |
| $R_a$                       | air gas constant.  |

The relationship between specific humidity ratio ( $w$ ) and specific humidity ratio on a mole basis ( $\omega$ ) is expressed as  $\omega = 1.608\omega$  [60]. The specific humidity ratio is calculated using the following [61]

$$\omega = 0.622 \times \frac{p_v}{p_{atm} - p_v} \text{ where } p_v = \phi \times P_{sat} \quad (14)$$

where:

|        |                                      |
|--------|--------------------------------------|
| $p_v$  | partial pressure.                    |
| $\Phi$ | relative humidity assumed to be 60%. |

The specific humidity ratio ( $w$ ) is  $4.62 \times 10^{-3}$  at 10 °C and the specific humidity at the reference environment conditions ( $w_0$ ) is 0.0163 at 30 °C. Additionally, Equation (12) can be rewritten as follows:

$$X_{water\_vapour\_mixture} = \left( C_{p,a} + \omega C_{p,v} \right) T_0 \left( \frac{T}{T_0} - 1 - \ln \frac{T}{T_0} \right) (1 + 1.608\omega) R_a T_0 \ln \frac{P}{P_0} + R_a T_0 \left( (1 + 1.608\omega) \ln \left[ \frac{1 + 1.608\omega_0}{1 + 1.608\omega} \right] + 1.608\omega \ln \frac{\omega}{\omega_0} \right) \quad (15)$$

The water expansion exergy ( $X_{water\_vapor\_mixture}$ ) is calculated to be 1.486 kJ/kg. Considering that the mass of water exiting the system due to expansion is 0.104 kg, as discussed in Section 2.2.2, the resulting water expansion exergy is 0.154 kJ. Over a 4-h period, the rate of water expansion exergy is 0.011 W. The relative exergy associated with water expansion compared to solar exergy ( $\frac{X_{Water\_expansion}}{X_{Solar}}$ ) is  $1.77 \times 10^{-5}$ , making it negligible when compared to solar exergy.

#### 2.4.7. Water Expansion Due to Transpiration

The amount of water transpired is equal to the amount of water entering the crop system from the ground surface. The exergy associated with water transpiration is calculated using the following:

$$X_{Water\_transpiration} = \dot{m}_{out} \times [(h_{in} - h_{out}) - T_0(S_{in} - S_{out})] \quad (16)$$

where:

|                            |  |
|----------------------------|--|
| $X_{water\_transpiration}$ | exergy associated with water expansion due to transpiration. |
| $h_0$                      | enthalpy at the reference environmental temperature.         |

The water transpiration exergy ( $X_{\text{water\_transpiration}}$ ) is determined to be 17.1 W with a relative water transpiration exergy ( $\frac{X_{\text{Water\_transpiration}}}{X_{\text{Solar}}}$ ) of 0.028. This indicates that the exergy contribution from water transpiration is small (2.8%) compared to solar exergy.

### 3. Results

As outlined in the Materials and Methods section, it is evident that not all terms have the same order of magnitude. Consequently, not all terms discussed in Equation (1) are significant for thermal measurements conducted during midday conditions at the Elora, ON, Canada location. Table 1 provides a summary of the energy terms, highlighting the identification of relevant and negligible terms in the energy balance for a crop plant system based on the Elora, Ontario case study.

**Table 1.** Energy contribution by source.

| Energy Term                                     | Energy Term Magnitude in Comparison to Measured Radiation | Assumptions and Approximations   |
|---|---|--|
| Work ( $\int PdV$ )                             | Zero <sup>1</sup>   | No volume change. Pressure changes are irrelevant.   |
| Air and water expansion                         | Negligible  | Assuming ideal gas over 4-h period of heating from coolest to warmest crop plant temperature (i.e., morning to afternoon).   |
| Fertilizer input                                | Zero  | Fertilizer is applied either once or periodically. Since fertilizer was not applied on the day temperature measurements were conducted, the “rate” of energy flow from fertilizer during the measurement period is zero. It is important to note that Equation (2) represents a rate equation. |
| Water transpiration                             | Order of 102 W/m <sup>2</sup>                             | Assumptions are listed in Section 2.2.3.   |
| Biomass output                                  | Zero  | Zero prior to harvest when temperature measurements were taken.  |
| Soil conduction heat flux                       | Small   | Assumptions are listed in Section 2.2.5  |
| Emitted radiation                               | [400–700 W/m <sup>2</sup> ]                               | Measured during midday conditions.   |
| Reflected radiation                             | [80–120 W/m <sup>2</sup> ]                                | Measured during midday conditions.   |
| Background radiation (5–30 $\mu\text{m}$ )      | [350–500 W/m <sup>2</sup> ]                               | Measured during midday conditions.   |
| Incoming solar radiation (0.3–2 $\mu\text{m}$ ) | [400–900 W/m <sup>2</sup> ]                               | Measured during midday conditions.   |

<sup>1</sup> By definition, there is no change in the system volume (V); therefore,  $dV = 0$  at all times of the day, resulting in zero work transfer.

Table 1 shows that all the radiation and transpiration terms in Equation (2) dominate the other energy flow terms. For exergy analysis, not all the terms in Equation (7) are significant for thermal measurements taken during midday conditions. The exergy terms and their respective significance are summarized in Table 2, which outlines the identification of relevant and negligible terms in the exergy balance for a crop plant system at the Elora, ON, Canada case study location.

In conclusion, as shown in Table 2, solar exergy dominates all other exergy input and output flow terms, with the majority of solar exergy either being destroyed or utilized by the system through various processes, such as photosynthesis and transpiration. Additionally, according to Equation (8), solar exergy can only be modified by changing the surface temperature, assuming a constant solar temperature.

**Table 2.** Exergy contribution by source.

| Exergy Term             | Approximate Exergy Term Magnitude in Comparison to Solar Exergy  | Assumptions and Approximations   |
|-------------------------|--|--|
| Work term $\int PdV$    | No change in the system volume (V). Therefore, exergy transfer is zero   | No volume change. Pressure changes are irrelevant  |
| Air and water expansion | Negligible   | For more details, please refer Sections 2.4.5 and 2.4.6  |
| Fertilizer input        | Negligible   | Assumptions: Average solar plus background flux in the Elora, Canada is 1325 W/m <sup>2</sup> , over 1 m <sup>2</sup> area, growing season of 3 months, 10 h sunlight per day, and the fertilizer is ammonium nitrate. For more details, please refer to Section 2.4.3 |
| Water transpiration     | Small order of 0.012% compared to solar exergy   | For more details, please refer to Section 2.4.7  |
| Biomass output          | Zero   | Zero prior to harvest when temperature measurements were taken   |
| Soil conduction         | Small order of 0.088% compared to solar exergy   | For more details, refer to Section 2.4.4   |
| Background radiation    | The exergy ratio is 0.0163 and $1.17 \times 10^{-3}$ for background temperatures of 1 °C and 18 °C, respectively | The exergy contribution from background radiation for assumed background temperatures of 1 °C and 18 °C ranges from small (1.2%) to negligible (0.0828%), respectively. For more details, please refer to Section 2.4.2  |
| Solar radiation         | The solar exergy amount is 0.931   | By definition, the relative exergy is 1 ( $\frac{X_{Solar}}{X_{Solar}}$ ). For more details, please refer to Section 2.4.1   |

#### 4. Discussion

This study investigates energy and exergy flows in a crop plant system to identify the dominant flows affecting crop plant health and development. After conducting an energy balance analysis, it was found that radiation and transpiration dominate all other energy input and output flow terms. For the exergy balance, it was found that solar exergy is the dominant factor among all exergy input and output flow terms with the majority of solar exergy either being utilized or destroyed by the system through various processes, including photosynthesis and transpiration.

Exergy serves as an ecological indicator to evaluate ecosystem development, complexity, and integrity [24–31]. The incoming solar exergy is significantly greater in magnitude compared to the amount of exergy consumed by human activities. The sun provides approximately 13,000 times more exergy than what is utilized by humanity [8,20,21]. Solar exergy reaching the Earth's surface sustains life on Earth by driving photosynthesis in crop plant systems, which converts solar energy into chemical energy [48]. Ecosystems evolve to enhance their capacity to survive in the environment by efficiently utilizing solar exergy from incoming radiation to sustain their internal organization. The greater the amount of solar exergy an ecosystem captures, the higher its capability to support organizational and survival functions [28–31]. Thus, ecosystem development can be assessed by measuring its rate of solar exergy utilization [48,49].

The exergy destruction principle is used to explain the relationship between crop surface temperature and crop stress. During the day, the solar exergy input significantly exceeds the exergy output [48,49], demonstrating a direct relationship between solar exergy and crop surface temperature as presented in Section 2.4.1. In this context, solar exergy can be altered solely by modifying the surface temperature, assuming a constant solar temperature. It was found that the available solar exergy to a crop plant system is maximized at lower surface temperatures based on the exergy analysis for a crop plant system [48,49]. Therefore, a crop system's health and development can be assessed using its surface temperature. This study highlights the significance of using crop surface temperature as an indicator of crop stress, as explained through an engineering thermodynamic principle (i.e., the exergy destruction principle). According to this principle (EDP), more developed and complex ecosystems, including crop plant system, exhibit lower surface temperatures during the day compared to less developed ecosystems [30,31,47–49]. Crop plant systems evolve to enhance their efficiency in exergy degradation, as shown by surface temperature measurements, which are consistent with the predictions of the exergy destruction principle [47–49]. Exergy destruction within a crop plant system is determined by the difference between incoming and outgoing exergy flows. The exergy of incoming radiation is the dominant component of these flows. Assuming that a crop plant system receives the same amount of incoming solar energy (i.e., under identical field conditions and environmental parameters), less stressed and more developed crops will emit energy at a lower exergy level, resulting in a lower surface temperature compared to stressed and less developed crops. Therefore, crop surface temperature can be utilized as a primary indicator of the exergy available to a crop plant system.

## 5. Conclusions

The results obtained from this work indicate that the temperate zone midday radiation energy and exergy flows govern crop surface temperature, thus supporting the sole use of crop surface temperature as a possible tool to detect crop stress at a first-order level. As a recommendation, future work should refine the set of assumptions applied in energy and exergy analysis presented in this paper to cover a wider range of climate zones and improve the understanding of when soil and environment temperature should be considered if crop surface temperature is used to detect crop stress.

Future considerations should be expanded to include the calculation of cumulative exergy for crop yield production and the exergy related to soil and plant interaction. In addition, different internal mechanisms (e.g., evapotranspiration, respiration, etc.) should be explored to investigate their direct effects on crop stress. Future work will also focus on testing the current model with different crop types under various climatic conditions.

**Author Contributions:** H.A. and R.F. contributed to the hypothesis formulation of the research, analyzing, discussing the results, and manuscript writing. All authors have read and agreed to the published version of the manuscript.

**Funding:** This research is funded by the Natural Sciences and Engineering Research Council of Canada (NSERC).

**Data Availability Statement:** Data are contained within the article.

**Acknowledgments:** This research was undertaken in part with funding from the Canada First Research Excellence Fund and through Growing Forward 2 (GF2), a federal–provincial–territorial initiative. The Agricultural Adaptation Council assists in the delivery of GF2 in Ontario, Canada. The authors would also like to acknowledge the support of the Natural Sciences and Engineering Research Council of Canada (NSERC).

**Conflicts of Interest:** The authors declare no conflicts of interest.

## References

1. Cengel, Y.A.; Boles, M.A.; Kanoğlu, M. *Thermodynamics: An Engineering Approach*; McGraw-Hill: New York, NY, USA, 2011; Volume 5, p. 445.
2. Burk, D.; Cornfield, J.; Schwartz, M. The efficient transformation of light into chemical energy in photosynthesis. *Sci. Mon.* **1951**, *73*, 213–223.
3. Ortega-Farias, S.O. A Comparative Evaluation of Residual Energy Balance, Penman, and Penman-Monteith Estimates of Daytime Variation of Evapotranspiration. Ph.D. Thesis, Oregon State University, Corvallis, OR, USA, 1993.
4. Duan, Z.; Grimmond, C.S.; Gao, C.Y.; Sun, T.; Liu, C.; Wang, L.; Gao, Z. Seasonal and interannual variations in the surface energy fluxes of a rice–wheat rotation in Eastern China. *J. Appl. Meteorol. Climatol.* **2021**, *60*, 877–891. [[CrossRef](#)]
5. Stoy, P.C.; Mauder, M.; Foken, T.; Marcolla, B.; Boegh, E.; Ibrom, A.; Varlagin, A. A data-driven analysis of energy balance closure across FLUXNET research sites: The role of landscape scale heterogeneity. *Agric. For. Meteorol.* **2013**, *171*, 137–152. [[CrossRef](#)]
6. Bejan, A. *Advanced Engineering Thermodynamics*; John Wiley and Sons: Hoboken, NJ, USA, 2016.
7. Gaudreau, K. Exergy Analysis and Resource Accounting. Master’s Thesis, University of Waterloo, Waterloo, ON, Canada, 2009.
8. Wall, G. *Exergy—A Useful Concept Within Resource Accounting*; Chalmers Tekniska Högskola, Göteborgs Universitet: Göteborg, Sweden, 1977.
9. Valero, A. Exergy accounting: Capabilities and drawbacks. *Energy* **2006**, *31*, 164–180. [[CrossRef](#)]
10. Valero, A. Exergy Evolution of the Mineral Capital on Earth. Ph.D. Thesis, Mechanical Engineering, University of Zaragoza, Zaragoza, Spain, 2008; p. 481.
11. Rosen, M.A.; Dincer, I.; Kanoğlu, M. Role of exergy in increasing efficiency and sustainability and reducing environmental impact. *Energy Policy* **2008**, *36*, 128–137. [[CrossRef](#)]
12. Dincer, I.; Rosen, M.A. *Exergy—Energy, Environment and Sustainable Development*; Elsevier: Oxford, UK, 2007.
13. Dincer, I.; Rosen, M.A. Exergy in policy development and education. In *Exergy—Energy, Environment and Sustainable Development*; Elsevier: Oxford, UK, 2007.
14. Kotas, T.J. *The Exergy Method of Thermal Plant Analysis*; Elsevier: Oxford, UK, 2013.
15. Schneider, E.D.; Kay, J.J. Life as a manifestation of the second law of thermodynamics. *Math. Comput. Model.* **1994**, *19*, 25–48. [[CrossRef](#)]
16. Schneider, E.D.; Kay, J.J. Complexity and thermodynamics: Towards a new ecology. *Futures* **1994**, *26*, 626–647. [[CrossRef](#)]
17. Kay, J. Ecosystems as self-organizing holarchic open systems. In *Handbook of Ecosystems Theories and Management*; CRS Press: Boca Raton, FL, USA, 2000.
18. Cornelissen, R.L. Thermodynamics and Sustainable Development—The Use of Exergy Analysis and the Reduction of Irreversibility. Ph.D. Thesis, Mechanical Engineering, University of Groningen, Groningen, The Netherlands, 1997; p. 170.
19. Cornelissen, R.L.; Hirs, G.G. The value of the exergetic life cycle assessment besides the LCA. *Energy Convers. Manag.* **2002**, *43*, 1417–1424. [[CrossRef](#)]
20. Wall, G. Exergy conversion in the Swedish society. *Resour. Energy* **1987**, *9*, 55–73. [[CrossRef](#)]
21. Wall, G. Exergy conversion in the Japanese society. *Energy* **1990**, *15*, 435–444. [[CrossRef](#)]
22. Maes, W.; Pashuysen, T.; Trabucco, A.; Veroustraete, F.; Muys, B. Does energy dissipation increase with ecosystem succession? Testing the ecosystem exergy theory combining theoretical simulations and thermal remote sensing observations. *Ecol. Model.* **2011**, *222*, 3917–3941. [[CrossRef](#)]
23. Silow, E.A.; Mokry, A.V.; Jørgensen, S.E. Some applications of thermodynamics for ecological systems. In *Thermodynamics-Interaction Studies-Solids, Liquids and Gases*; IntechOpen: Rijeka, Croatia, 2011.
24. Fraser, R.; Kay, J.J. Exergy analysis of ecosystems: Establishing a role for thermal remote sensing. In *Thermal Remote Sensing in Land Surface Processes*; Quattrochi, D., Luvall, J., Eds.; CRC Press: Boca Raton, FL, USA, 2004; pp. 283–360.
25. Kay, J.; Allen, T.; Fraser, R.; Luvall, J.; Ulanowicz, R. Can we use energy based indicators to characterize and measure the status of ecosystems, human, disturbed and natural. In Proceedings of the International Workshop: Advances in Energy Studies: Exploring Supplies, Constraints and Strategies, Porto Venere, Italy, 23–27 May 2001; SGE Editoriali Padova: Padova, Italy, 2001; pp. 121–133.
26. Kay, J. *The Ecosystem Approach: Complexity, Uncertainty, and Managing for Sustainability*; Columbia University Press: New York, NY, USA, 2008.
27. Holbo, H.; Luvall, J. Modeling surface temperature distributions in forest landscapes. *Remote Sens. Environ.* **1989**, *27*, 11–24. [[CrossRef](#)]
28. Quattrochi, D.A.; Luvall, J.C. *Thermal Remote Sensing in Earth Science Research*; SAGE Publications Ltd.: London, UK, 2009.
29. Luvall, J.; Holbo, H. Measurements of short-term thermal responses of coniferous forest canopies using thermal scanner data. *Remote Sens. Environ.* **1989**, *27*, 1–10. [[CrossRef](#)]

30. Luvall, J.C.; Rickman, D.; Fraser, R. Thermal remote sensing and the thermodynamics of ecosystem development. In *AGU Fall Meeting Abstracts*; American Geophysical Union: Washington, DC, USA, 2013.
31. Quattrochi, D.A.; Luvall, J.C. *Thermal Remote Sensing in Land Surface Processing*; CRC Press: Boca Raton, FL, USA, 2004.
32. Rock, G. *Energymetrics and the Development of Energy Analysis Tools*. Master's Thesis, Chalmers University of Technology, Göteborg, Sweden, 2012.
33. Marques, J.G.; Costa, A.L.; Pereira, C. Gibbs free energy ( $\Delta G$ ) analysis for the NaOH (sodium-oxygen-hydrogen) thermochemical water splitting cycle. *Int. J. Hydrogen Energy* **2019**, *44*, 14536–14549. [[CrossRef](#)]
34. Szargut, J. *Exergy Method: Technical and Ecological Applications*; WIT Press: Cambridge, MA, USA, 2005; Volume 18.
35. Yildizhan, H.; Taki, M. Assessment of tomato production process by cumulative exergy consumption approach in greenhouse and open field conditions: Case study of Turkey. *Energy* **2018**, *156*, 401–408. [[CrossRef](#)]
36. Hoang, V.N.; Rao, D.P. Measuring and decomposing sustainable efficiency in agricultural production: A cumulative exergy balance approach. *Ecol. Econ.* **2010**, *69*, 1765–1776. [[CrossRef](#)]
37. Kirova-Yordanova, Z. Cumulative Exergy Concept: Keystone to the Exergy Method Application in Chemical Industry In memory of Professor Jan Szargut. In Proceedings of the 31st International Conference on Efficiency, Cost, Optimization, Simulation and Environmental Impact of Energy Systems, Guimarães, Portugal, 17–22 June 2018.
38. Flórez-Orrego, D.; Henriques, I.B.; Nguyen, T.V.; da Silva, J.A.M.; Mady, C.E.K.; Pellegrini, L.F.; de Oliveira Junior, S. The contributions of Prof. Jan Szargut to the exergy and environmental assessment of complex energy systems. *Energy* **2018**, *161*, 482–492. [[CrossRef](#)]
39. Giampietro, M. From input–output analysis to the quantification of metabolic patterns: David Pimentel's contribution to the analysis of complex environmental problems. *Environ. Dev. Sustain.* **2024**, *26*, 29911–29932. [[CrossRef](#)]
40. Biofuels, T.W. Solar and wind as renewable energy systems. In *Benefits and Risks*; Springer: New York, NY, USA, 2008; pp. 153–171.
41. Prigogine, I.; Glansdorff, P. *Thermodynamic Theory of Structure, Stability and Fluctuations Structure, Stability and Fluctuations*; Wiley-Interscience: Hoboken, NJ, USA, 1971.
42. Prigogine, I.; Ji, S. *Schrödinger and the Riddle of Life Molecular Theories of Cell Life and Death*; Rutgers University Press: New Brunswick, NJ, USA, 1991.
43. Prigogine, I.; Wiame, J.-M. Biologie et thermodynamique des phénomènes irréversibles. *Experientia* **1946**, *2*, 451–453. [[CrossRef](#)] [[PubMed](#)]
44. Righetto, F.G.; Mady, C.E.K. Exergy Analysis of a Sugarcane Crop: A Planting-to-Harvest Approach. *Sustainability* **2023**, *15*, 14686. [[CrossRef](#)]
45. Jekayinfa, S.O.; Adeleke, K.M.; Ogunlade, C.A.; Sasanya, B.F.; Azeez, N.A. Energy and exergy analysis of Soybean production and processing system. *Clean. Eng. Technol.* **2022**, *10*, 100540. [[CrossRef](#)]
46. Nikkhah, A.; Kosari-Moghaddam, A.; Troujeni, M.E.; Bacenetti, J.; Van Haute, S. Exergy flow of rice production system in Italy: Comparison among nine different varieties. *Sci. Total Environ.* **2021**, *781*, 146718. [[CrossRef](#)] [[PubMed](#)]
47. Alzaben, H.; Fraser, R.; Swanton, C. An inverse correlation between corn temperature and nitrogen stress: A field case study. *Agronomy* **2019**, *111*, 3207–3219. [[CrossRef](#)]
48. Alzaben, H. Investigating the Exergy Destruction Principle Applied to Precision Agriculture Using Thermal Remote Sensing. Ph.D. Thesis, University of Waterloo, Waterloo, ON, Canada, 2020.
49. Alzaben, H.; Fraser, R.; Swanton, C. The Role of Engineering Thermodynamics in Explaining the Inverse Correlation between Surface Temperature and Supplied Nitrogen Rate in Corn Plants: A Greenhouse Case Study. *Agriculture* **2021**, *11*, 101. [[CrossRef](#)]
50. Ratliff, L.F.; Ritchie, J.T.; Cassel, D.K. Field-measured limits of soil water availability as related to laboratory-measured properties 1. *Soil Sci. Soc. Am. J.* **1983**, *47*, 770–775. [[CrossRef](#)]
51. Bhatt, R.; Hossain, A. Concept and consequence of evapotranspiration for sustainable crop production in the era of climate change. *Adv. Evapotranspiration Methods Appl.* **2019**, *1*, 1–13.
52. Sansom, A. *Water in Texas: An Introduction*; University of Texas Press: Austin, TX, USA, 2008.
53. Lizotte, P.L.; Savoie, P.; De Champlain, A. Ash content and calorific energy of corn stover components in Eastern Canada. *Energies* **2015**, *8*, 4827–4838. [[CrossRef](#)]
54. Anapalli, S.S.; Green, T.R.; Reddy, K.N.; Gowda, P.H.; Sui, R.; Fisher, D.K.; Moorhead, J.E.; Marek, G.W. Application of an energy balance method for estimating evapotranspiration in cropping systems. *Agric. Water Manag.* **2018**, *204*, 107–117. [[CrossRef](#)]
55. Kabelac, S. *Thermodynamik der Strahlung*; Vieweg+Teubner Verlag: Wiesbaden, Germany, 1994.
56. Measuring the Temperature of the Sky and Clouds. Available online: <https://myasadata.larc.nasa.gov/sites/default/files/2018-12/Measuring%20the%20Temperature%20of%20the%20Sky%20and%20Clouds.pdf> (accessed on 22 September 2023).
57. McIntyre, J.H. Photovoltaic potential in the city of Guelph. *Guelph Eng. J.* **2008**, *1*, 24–26.
58. De Beer, J. *Potential for Industrial Energy-Efficiency Improvement in the Long Term*; Springer Science & Business Media: Berlin/Heidelberg, Germany, 2013; Volume 5.

59. Syngenta Corn Herbicide Portfolio. Available online: <https://www.syngenta-us.com/herbicides/callisto> (accessed on 30 December 2024).
60. Qureshi, B.A.; Zubair, S.M. Application of exergy analysis to various psychrometric processes. *Int. J. Energy Res.* **2003**, *27*, 1079–1094. [[CrossRef](#)]
61. Salazar-Pereyra, M.; Toledo-Velázquez, M.; Eslava, G.T.; Lugo-Leyte, R.; Rosas, C.R. Energy and exergy analysis of moist air for application in power plants. *Energy Power Eng.* **2011**, *3*, 376–381. [[CrossRef](#)]

**Disclaimer/Publisher’s Note:** The statements, opinions and data contained in all publications are solely those of the individual author(s) and contributor(s) and not of MDPI and/or the editor(s). MDPI and/or the editor(s) disclaim responsibility for any injury to people or property resulting from any ideas, methods, instructions or products referred to in the content.